JACS
JOURNAL OF THE AMERICAN CHEMICAL SOCIETY

Subscriber access provided by American Chemical Society

Article

Evidence for a Two-Step Mechanism in Electronically Selective Single-Walled Carbon Nanotube Reactions

Monica L. Usrey, Ethan S. Lippmann, and Michael S. Strano

J. Am. Chem. Soc., **2005**, 127 (46), 16129-16135• DOI: 10.1021/ja0537530 • Publication Date (Web): 28 October 2005

Downloaded from http://pubs.acs.org on March 25, 2009

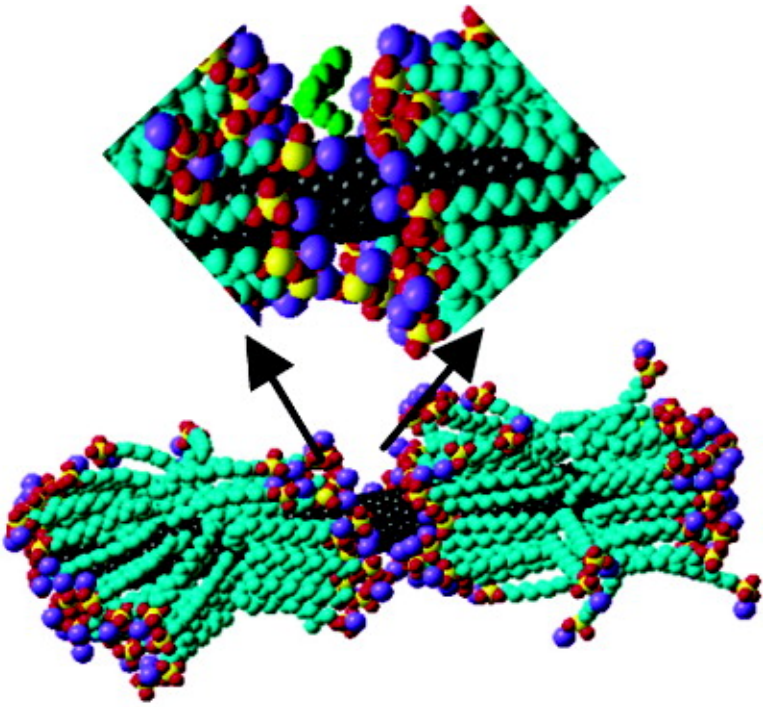

More About This Article

Additional resources and features associated with this article are available within the HTML version:

- Supporting Information
- Links to the 12 articles that cite this article, as of the time of this article download
- Access to high resolution figures
- Links to articles and content related to this article
- Copyright permission to reproduce figures and/or text from this article

ACS Publications
High quality. High impact.

Journal of the American Chemical Society is published by the American Chemical Society. 1155 Sixteenth Street N.W., Washington, DC 20036

JACS
JOURNAL OF THE AMERICAN CHEMICAL SOCIETY

Subscriber access provided by American Chemical Society

View the Full Text HTML

ACS Publications
High quality. High impact.

Journal of the American Chemical Society is published by the American Chemical Society. 1155 Sixteenth Street N.W., Washington, DC 20036

J|A|C|S
ARTICLES
Published on Web 10/28/2005

Evidence for a Two-Step Mechanism in Electronically Selective Single-Walled Carbon Nanotube Reactions

Monica L. Usrey, Ethan S. Lippmann, and Michael S. Strano*

Contribution from the Department of Chemical and Biomolecular Engineering, University of Illinois—Urbana/Champaign, Urbana, Illinois 61801

Received June 8, 2005; E-mail: strano@uiuc.edu

Abstract: Covalent and noncovalent chemistries that are selective to single-walled carbon nanotubes of a particular electronic type have become increasingly important for electronic structure separation and on-chip modification of nanoelectronic devices. By monitoring transient Raman spectroscopy and photoluminescence (PL) during a reaction with 4-chlorobenzene diazonium in aqueous solution, evidence for a characteristic two-step mechanism with two distinct time constants is uncovered. A long-lived intermediate selectively and noncovalently binds and partially dopes the nanotube surface ($\tau = 2.4$ min). A slower, covalent reaction is tracked using the time-dependent increase in the disorder mode in Raman ($\tau = 73$ min). The transient Raman and PL data are well described using a series of two first-order reactions. The covalent bonding step can be deactivated by changing the structure of the surfactant adsorbed phase, further supporting the mechanism.

Introduction

Single-walled carbon nanotubes (SWNT) possess highly unique electronic, mechanical, and optical properties, making them the subject of intense study since their discovery in 1993 by Iijima.[1] Individual carbon nanotubes are semiconducting or metallic in nature, depending upon their chirality.[2−4] Synthetic methods invariably produce polydisperse mixtures of semiconducting and metallic nanotubes. This limits applications in nanoelectronics and other areas. Efforts to separate these polydisperse mixtures into semiconducting and metallic components[5−9] have yet to conclusively demonstrate preparative separation. Chemical modification of electrical properties[10,11] has been pursued with some success.

The first electronic structure selective chemistry used a 4-chlorobenzene diazonium salt to selectively react metallic over semiconducting nanotubes.[12,13] Researchers extended this same chemistry to the modification of nanotube field effect transistors in order to improve the ratio of current between on and off states.[10,11] In addition to nanoelectronic applications, these chemistries may lead to routes for the preparative separation of metallic and semiconducting carbon nanotubes.[7,8,14] The possible mechanistic pathways of the diazonium/SWNT reaction have been studied using GC−MS and XPS analysis of the reaction products.[15]

If the reaction is viewed as one between the nanotube macromolecule and a single reactant, this selectivity presents some theoretical problems. Carbon nanotubes are metallic or semiconducting, based upon delocalized electrons occupying a 1-D density of states. However, any covalent bond is necessarily broken and formed between localized electrons. In the vicinity of localized electrons, the SWNT can no longer be described using a band model that assumes delocalized electrons moving in a periodic potential. Zhao and co-workers used density functional calculations to show that while covalent bonding induces an impurity state with a relatively delocalized wave function, the covalent linkage itself is a highly localized event.[16,17] Therefore, in an electronically selective reaction, how does the reagent detect a metallic or semiconducting species when the localization of electrons necessary for covalent bonding eliminates the distinction between these types?

(1) Iijima, S.; Ichihashi, T. *Nature* **1993**, *363*, 603−605.
(2) Dresselhaus,M. S.; Dresselhaus, G.; Eklund, P. C. *Science of fullerenes and carbon nanotubes*; Academic Press: San Diego, 1996.
(3) Saito, R.; Dresselhaus, G.; Dresselhaus, M. S. *Physical Properties of Carbon Nanotubes*; Imperial College Press: London, 1999.
(4) Dresselhaus, M. S.; Dresselhaus, G.; Avouris, P. *Carbon Nanotubes: Synthesis, Structure, Properties, and Applications*; Springer-Verlag: Heidelberg, Germany, 2001; Vol. 80.
(5) Chattopadhyay, D.; Galeska, L.; Papadimitrakopoulos, F. *J. Am. Chem. Soc.* **2003**, *125*, 3370−3375.
(6) Samsonidze, G. G.; Chou, S. G.; Santos, A. P.; Brar, V. W.; Dresselhaus, G.; Dresselhaus, M. S.; Selbst, A.; Swan, A. K.; Unlu, M. S.; Goldberg, B. B.; Chattopadhyay, D.; Kim, S. N.; Papadimitrakopoulos, F. *Appl. Phys. Lett.* **2004**, *85*, 1006−1008.
(7) Krupke, R.; Hennrich, F.; von Lohneysen, H.; Kappes, M. M. *Science* **2003**, *301*, 344−347.
(8) Chen, Z. H.; Du, X.; Du, M. H.; Rancken, C. D.; Cheng, H. P.; Rinzler, A. G. *Nano Lett.* **2003**, *3*, 1245−1249.
(9) Dyke, C. A.; Stewart, M. P.; Tour, J. M. *J. Am. Chem. Soc.* **2005**, *127*, 4497−4509.
(10) An, L.; Fu, Q. A.; Lu, C. G.; Liu, J. *J. Am. Chem. Soc.* **2004**, *126*, 10520−10521.
(11) Balasubramanian, K.; Sordan, R.; Burghard, M.; Kern, K. *Nano Lett.* **2004**, *4*, 827−830.
(12) Strano, M. S. *J. Am. Chem. Soc.* **2003**, *125*, 16148−16153.
(13) Strano, M. S.; Dyke, C. A.; Usrey, M. L.; Barone, P. W.; Allen, M. J.; Shan, H. W.; Kittrell, C.; Hauge, R. H.; Tour, J. M.; Smalley, R. E. *Science* **2003**, *301*, 1519−1522.
(14) Baik, S.; Usrey, M.; Rotkina, L.; Strano, M. *J. Phys. Chem. B* **2004**, *108*, 15560−15564.
(15) Dyke, C. A.; Stewart, M. P.; Maya, F.; Tour, J. M. *Synlett* **2004**, 155−160.
(16) Park, H.; Zhao, J.; Lu, J. P. *Nanotechnology* **2005**, *16*, 635−638.
(17) Zhao, J. J.; Park, H. K.; Han, J.; Lu, J. P. *J. Phys. Chem. B* **2004**, *108*, 4227−4230.

10.1021/ja0537530 CCC: $30.25 © 2005 American Chemical Society

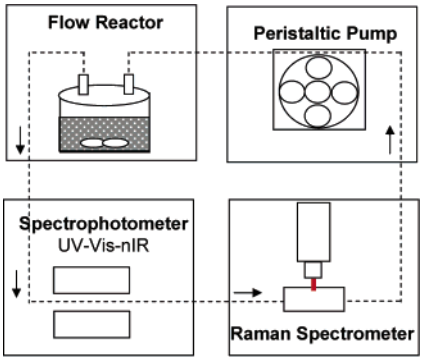

Figure 1. Diagram of flow-through reactor setup: 70 mL of SDS/SWNT solution (pH 11) is contained in a well-stirred 70- × 50-mm Pyrex crystallizing dish; 0.0076 mM additions of 4-chlorobenzene diazonium are made at 60−90-min intervals. During the reaction, material is continuously drawn through tubing connected to a UV−vis−NIR spectrophotometer and Raman spectrometer by a peristaltic pump. Absorption spectra (190−1900 nm) are taken at the steady-state point prior to each addition. Raman spectra are obtained every 10 s to monitor the G peak and D peak transient behavior.

In this work, we answer this question by exploring the mechanism of electronically selective reactions in carbon nanotubes with a dual purpose: to assist in the practical development of SWNT chemistries and separation methods, and to address the mismatch between local and delocalized views of electron transfer. We show that selectivity proceeds by two distinct and long-lived mechanistic steps: a selective noncovalent adsorption followed by a slower covalent reaction that need not be selective. Transient Raman, photoluminescence (PL), and photoabsorption spectroscopy measurements during the reaction show evidence of this mechanism. X-ray photoelectron spectroscopy (XPS) is used to estimate the extent of functionalization (moles of chlorine per mole of carbon) under complete and selective reaction conditions. Conducting the reaction in a different surfactant system (sodium cholate) is shown to eliminate the covalent pathway but preserve the selectivity, supporting the proposed mechanism.

Experimental Section

Suspension of SWNTs. HiPco nanotubes (Rice University) were suspended in 1 wt % sodium dodecyl sulfate (SDS, Sigma Aldrich) or 2 wt % sodium cholate (Sigma Aldrich) in deuterated aqueous solution according to an established procedure.[18] Deuterated water (D_2O) was used to eliminate water absorption features in the SWNT solution UV−vis−NIR absorption spectra.

Synthesis of 4-Chlorobenzene Diazonium Reagent. The 4-chlorobenzene diazonium tetrafluoroborate salt was synthesized by reacting equimolar quantities of 4-chloroaniline (Sigma Aldrich) and nitrosyl tetrafluoroborate (Sigma Aldrich) in acetonitrile solvent. The reaction was conducted at −20 °C (dry ice/isopropyl alcohol bath) under nitrogen. The diazonium salt was precipitated with diethyl ether, filtered, dried, and stored under nitrogen at −20 °C. Prior to the reaction, a 5.31 mM solution of the 4-chlorobenzene diazonium salt in D_2O was prepared. The aqueous solution was stored in the dark at 4 °C to reduce decomposition of the diazonium salt.

Selective Reaction Setup. The selective reaction was conducted in a custom-made flow reactor setup (Figure 1). The reactor vessel is a well-stirred 70- × 50-mm Pyrex crystallizing dish with a custom-made Kevlar lid fitted with tubing ports. A MasterFlex L/S Economy Drive peristaltic pump with Easy Load II rotor head pumped the reaction solution through 1/8-in. o.d. (1/16 in. thickness) Tygon tubing. A minimum flow rate was maintained to prevent generation of SDS/air bubbles in the reactor vessel and tubing which would disrupt both the absorption and Raman spectra. The solution flowed from the reactor vessel to the UV−vis−NIR spectrophotometer to the Raman spectrometer using Starna quartz flow-through cuvettes. The UV−vis−NIR spectrophotometer used in this study is a Shimadzu UV-3101PC. Absorption spectra were generated (190−1900 nm) at every steady-state point during the reaction (approximately every 60 min). The Raman spectrometer used is a Raman Rxn system from Kaiser Optical Systems using a 785-nm photodiode laser at 200 mW. Raman spectra, including photoluminescence, were generated every 10 s during the reaction. Prior to the reaction, the pH of the SWNT solution (1 wt % SDS/D_2O) was increased from 5.5 to 11 using NaOH solution (Sigma Aldrich). Three additions (0.0076 mM each) of 4-chlorobenzene diazonium were made at 0, 87, and 158 min, respectively.

Sodium Cholate Experiment. The sodium cholate experiment was conducted in a Starna quartz cuvette with UV−vis−NIR absorption spectra gathered (190−1900 nm) every 5 min. The pH of the SWNT solution (2 wt % cholate/D_2O) was increased from 5.5 to 11 using NaOH solution (Sigma Aldrich). Immediately before the experiment, a 9.38 mM solution of the 4-chlorobenzene diazonium salt in D_2O was prepared. A single addition of 1.25 mM was made to the cholate-suspended SWNT solution, and absorption spectra (190−1900 nm) were gathered every 5 min for 2.5 h. Initial and final Raman spectra were obtained at 200 mW using the Raman Rxn system.

XPS Analysis. X-ray photoelectron spectroscopy (XPS) data were gathered at the UIUC Center for Microanalysis of Materials. Solid samples were prepared by flocking SDS-suspended SWNTs from aqueous solution using acetone (Fisher Scientific), filtering via gravity through a standard filter cone, and washing with acetone and methanol (Fisher Scientific) to remove residual SDS and/or excess reagent. Samples were mounted on a stainless steel sample holder using double-sided carbon tape. Data for completely functionalized samples were obtained on a Physical Electronics PHI 5400 instrument (0−1100 eV binding energy). Data for raw SWNT material and selectively functionalized samples were obtained on a Kratos Axis Ultra instrument (0−1100 eV binding energy).

Molecular Modeling. Molecular models were generated using Hyperchem Professional Software (Release 7). Geometry optimization simulations for SDS assembled on a carbon nanotube surface were conducted using the Polak−Ribiere (conjugate gradient) method. The simulations ended once a root-mean-square (RMS) gradient of 0.15 kcal/Å-mol was reached.

Results

Figure 2 shows the dynamic responses of the Raman disorder mode (D peak, Figure 2a), the tangential mode (G peak, Figure 2b), and photoluminescence (PL, Figure 2c) of the (6,5) and (7,5) nanotubes after three 0.076 mM additions of 4-chlorobenzene diazonium reagent. Curiously, the responses show a wide range of time constants after each addition (arrows).

The disorder mode (D peak, 1300 cm^{-1}) is a symmetry-disallowed Raman mode associated with a double-resonance process. For probing SWNT chemistry, it is an exclusive measure of covalent reaction: as bonds in the carbon lattice are broken and re-formed with a covalent aryl chloride attachment, the absolute cross section of this mode increases.[19−21]

(18) O'Connell, M. J.; Bachilo, S. M.; Huffman, C. B.; Moore, V. C.; Strano, M. S.; Haroz, E. H.; Rialon, K. L.; Boul, P. J.; Noon, W. H.; Kittrell, C.; Ma, J. P.; Hauge, R. H.; Weisman, R. B.; Smalley, R. E. *Science* **2002**, *297*, 593−596.

(19) Kurti, J.; Zolyomi, V.; Gruneis, A.; Kuzmany, H. *Phys. Rev. B* **2002**, *65*, 165433 (1−9).

(20) Zolyomi, V.; Kurti, J.; Gruneis, A.; Kuzmany, H. *Phys. Rev. Lett.* **2003**, *90*, 157401 (1−4).

(21) Dillon, A. C.; Parilla, P. A.; Alleman, J. L.; Gennett, T.; Jones, K. M.; Heben, M. J. *Chem. Phys. Lett.* **2005**, *401*, 522−528.

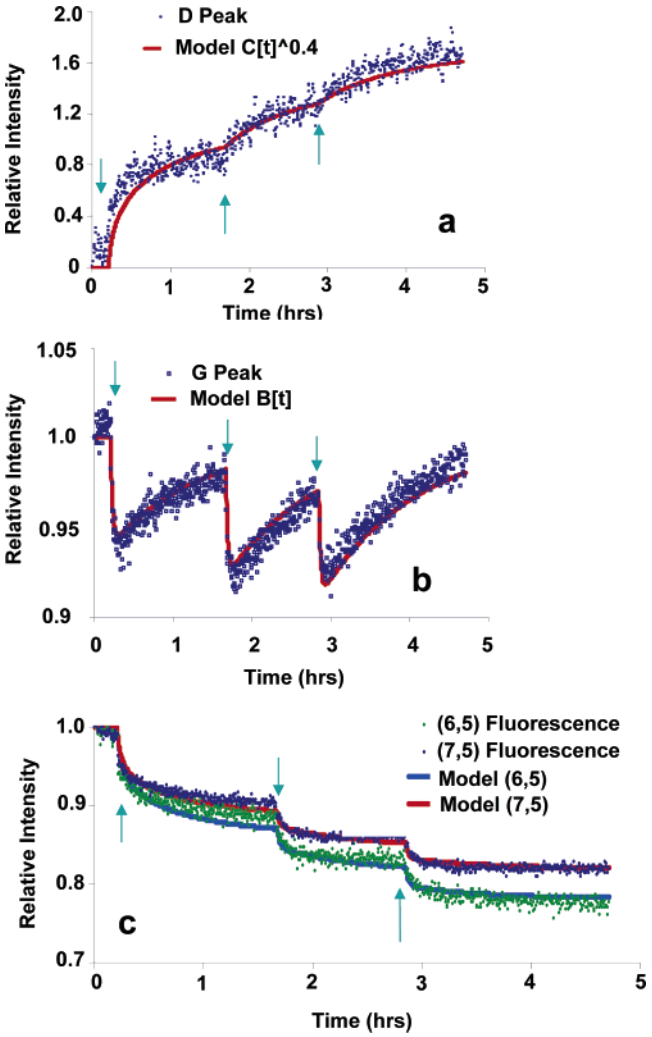

Figure 2. Raman transient data obtained during 4-chlorobenzene diazonium selective reaction. Arrows indicate addition points. Experimental data (scattered points) for the (a) disorder mode (D band), (b) tangential mode (G peak), and (c) (6,5) and (7,5) photoluminescence are compared to trends predicted by the mechanistic model (solid lines).

The extent of functionalization can be represented by the D/G intensity ratio, which allows the comparison of different samples or spectra taken at different excitation wavelengths.[21] Figure 2a shows that the D peak intensity increases monotonically in a first-order process ($\tau = 73$ min) and approaches a steady state after each addition. The intensity change following an addition becomes smaller after subsequent additions.

The tangential mode (G peak, 1590 cm^{-1}), representing the C−C bond stretch of all graphitic species demonstrates a characteristically different response to reagent addition on two different time scales. Figure 2b demonstrates that immediately following an addition, a sharp diminution is observed ($\tau_1 =$ 2.4 min) followed by a slower partial recovery ($\tau_2 = 72.9$ min). The tangential mode is resonance enhanced, and processes that dope a SWNT inter-band transition resonant with the excitation laser can diminish its intensity.[22] The restoration rate appears to match the time scale of the D-peak increase.

The photoluminescent responses of two selected SWNTs, (6,5) and (7,5), are shown to decrease rapidly on a time scale

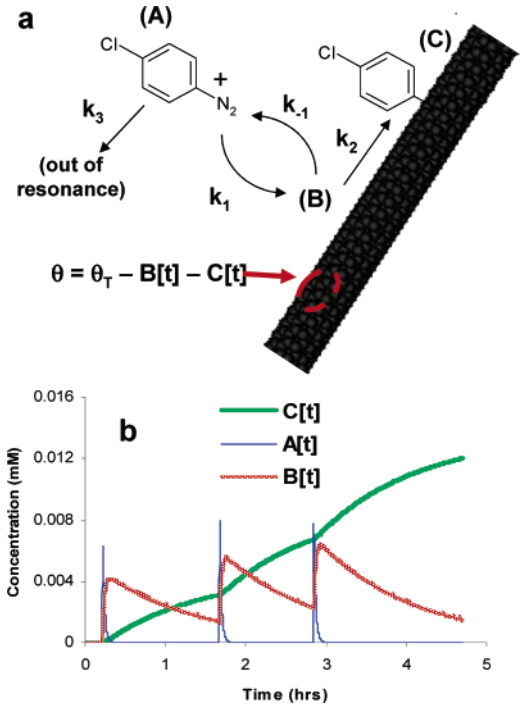

Figure 3. (a) Schematic of kinetic model displaying the three possible states of the diazonium reagent during the reaction: (A) free in solution, (B) adsorbed on nanotube surface, and (C) covalently bound to nanotube. (b) Predicted concentration profiles of A, B, and C diazonium states.

close to τ_1 with no subsequent restoration (Figure 2c). A total of four PL features were monitored; each demonstrates a similar response (Supporting Information). SWNT photoluminescence proceeds via an exciton recombination process and is sensitive to both adsorbed dopants and defects at the nanotube surface.

Developing an Approximate Kinetic Model. The transient behavior of the G peak suggests that a short-lived intermediate temporarily dopes the nanotube before its decay. This doping disproportionately diminishes the G peak intensity and reverses as the intermediate population is depleted by reaction. Compounds with aromatic structures similar to diazonium but without any charge (phenol, anisole, and 4-hydroxyaniline) were added under similar conditions with no response. This suggests that the positively charged diazonium itself may be responsible for the diminution. Upon physical adsorption within the surfactant phase around the nanotube, a partially transferred charge decreases the tangential mode slightly until covalent addition eliminates this adsorbed species. These changes could not be measured above experimental error (±8%) using photoabsorption, which is not as sensitive as low-background or background-free methods such as Raman and PL. The D peak responds to covalent addition, so the terminal step in the reaction should be related to its growth. The PL should respond to a combination of the two populations (adsorbed dopant and covalently bound moieties).[23]

We seek the simplest model capable of describing these changes, assuming first-order kinetics for both steps (Figure 3a). The diazonium reagent (A) first adsorbs noncovalently to an

(22) Strano, M. S.; Huffman, C. B.; Moore, V. C.; O'Connell, M. J.; Haroz, E. H.; Hubbard, J.; Miller, M.; Rialon, K.; Kittrell, C.; Ramesh, S.; Hauge, R. H.; Smalley, R. E. *J. Phys. Chem. B* **2003**, *107*, 6979−6985.

(23) Dukovic, G.; White, B. E.; Zhou, Z. Y.; Wang, F.; Jockusch, S.; Steigerwald, M. L.; Heinz, T. F.; Friesner, R. A.; Turro, N. J.; Brus, L. E. *J. Am. Chem. Soc.* **2004**, *126*, 15269−15276.

empty site (θ) on the nanotube surface, forming a charge-transfer complex (B). The diazonium group in this complex partially dopes the nanotube, diminishing the tangential mode in the Raman spectrum. This complex then decomposes to form a covalent bond with the nanotube surface (C). The resulting lattice defect increases the D band in the Raman spectrum.

$$A + \theta \underset{k_{-1}}{\overset{k_1}{\rightleftharpoons}} B \xrightarrow{k_2} C$$

The available sites on the nanotube (θ_T) are balanced by

$$\theta + B + C = (\theta_T)$$

In this work, the reaction is carried out at infinite dilution of the reagent. The resulting functionalization is sparse ($\theta[t] \gg (B[t] + C[t])$), and the system is pseudo-first order, with k_1 and k_2 representing the rate constants of the adsorption and reaction steps, respectively. Desorption is also negligible ($k_{-1} = 0$) in this case. Under these conditions, we can treat the SWNT as homogeneously solubilized reactive sites undergoing the following pseudo-first-order reaction A $\rightarrow$ B $\rightarrow$ C.

If the reaction is probed using resonant Raman spectroscopy, there are populations both in and out of resonance with the excitation laser.[24] The population outside the resonance window taking part in the reaction is modeled by a parallel first-order reaction with rate constant k_3 (A (k_3) $\rightarrow$ out of resonance), also shown in Figure 3a. The time-varying solution for B[t] with A[0] = A_o and B[0] = B_o,

$$B[t] = \frac{\exp[-k_2 t](B_o(k_1 - k_2 + k_3) - A_o(\exp[-(k_1 - k_2 + k_3)t] - 1)k_1)}{k_1 - k_2 + k_3}$$

exhibits a characteristic maximum after reagent addition. Figure 2b compares the experimental G peak response data with the regressed model trend with k_1, k_2, and k_3 equal to 24.7, 0.82, and 17.1 h^{-1}, respectively. The fraction of SWNT in resonance with the laser is proportional to the ratio of k_1 to the sum of k_1 and k_3. These empirical rate constants indicate that approximately 59% of all SWNT species in solution (metallic and semiconducting) are in resonance with the laser at 785 nm. Analysis of a revised Kataura plot for HiPco SWNT in aqueous solution indicates that only six semiconducting species are in resonance at 785 nm. Therefore, it is important to note that the above rate constants represent an average of all SWNT in the sample, with a disproportionate contribution from those in resonance.

The concentration of covalent defects, C[t], is C[t] = $\int_0^t k_2 B[t']\, dt'$. Figure 3b plots the concentrations of free diazonium A[t], adsorbed reagent B[t], and covalent ligand C[t] using the three parameters empirically determined above (k_1, k_2, k_3).

The population of covalently bound moieties should be related to the Raman D-band intensity, although no work to date has determined the functional dependence of the D-band intensity on actual defect concentration (C[t]). Several researchers have addressed its unique electronic dispersion and the nature of the complex two-phonon scattering process.[24,25] A linear relationship for oxidized SWNT bundles has been proposed.[26] The D-band (Figure 4a) cross section is dominated by a double-resonance process where an exciton decomposes into a phonon, scatters across the Brillouin zone, and may or may not encounter a defect.[19] If it does encounter a defect, the exciton can emit a photon of lower energy (as in this work). The mean free path of the excitation (i.e., the exciton) should play a strong role in this functional dependence. If the exciton is highly localized, the intensity of the D band is directly proportional to the probability of finding a defect or the concentration of defects, C[t]. However, Heinz and co-workers recently modeled SWNT excitons as having a radius several times the C−C bond length.[27] As the mean free path increases, this dependence becomes nonlinear and generally C[t]^n with $0 < n < 1$ (Supporting Information).

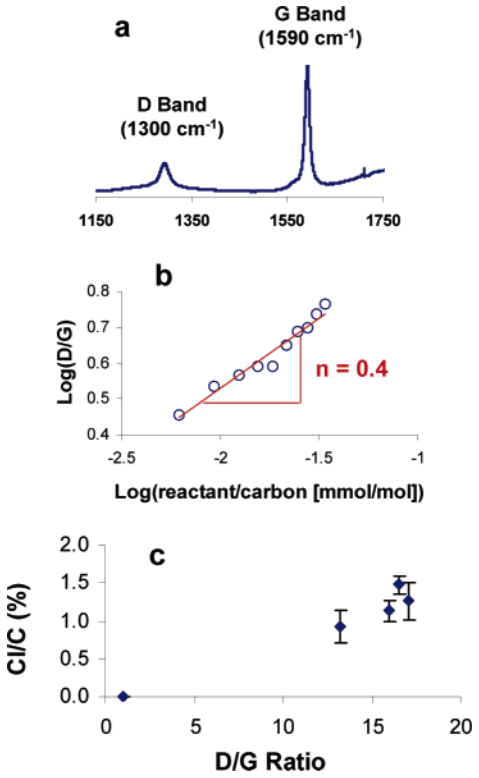

Figure 4. Transient behavior of the disorder mode (D peak) correlated to the extent of covalent reaction. (a) A sample Raman spectrum showing the disorder (D peak) and tangential (G peak) modes. (b) Plot of log(D/G ratio) versus log(mmol of reagent/mol of SWNT carbon) illustrating a linear logarithmic dependence. The slope of 0.4 indicates a 0.4-th order power dependence between extent of reaction and D/G ratio. (c) XPS results showing the ratio of %Cl to %C for five SWNT samples functionalized to increasing extents. This ratio is compared to the ratio of the D peak and G peak intensities.

To investigate this dependence empirically, a separate experiment was conducted where steady-state D peak and G peak intensities were measured as a function of total 4-chlorobenzene diazonium addition during a single selective reaction. Figure 4b illustrates a C[t]$^{0.4}$ dependence between the D/G ratio and the concentration of diazonium added. This C[t]$^{0.4}$ dependence

(24) Dresselhaus, M. S.; Dresselhaus, G.; Jorio, A.; Souza, A. G.; Saito, R. *Carbon* **2002**, *40*, 2043−2061.
(25) Souza, A. G.; Jorio, A.; Samsonidze, G. G.; Dresselhaus, G.; Saito, R.; Dresselhaus, M. S. *Nanotechnology* **2003**, *14*, 1130−1139.
(26) Kukovecz, A.; Kramberger, C.; Holzinger, M.; Kuzmany, H.; Schalko, J.; Mannsberger, M.; Hirsch, A. *J. Phys. Chem. B* **2002**, *106*, 6374−6380.
(27) Wang, F.; Dukovic, G.; Brus, L. E.; Heinz, T. F. *Science* **2005**, *308*, 838−841.

Table 1. Summary of XPS Analyses Conducted on SWNT Samples Representing (a) No Functionalization, (b) Selective Functionalization with 4-Chlorobenzene Diazonium, and (c) Complete, Nonselective Functionalization with 4-Chlorobenzene Diazonium

	XPS atomic analysis			mass balance
	%C	%O	%Cl	%Cl
no reaction	91.28 ± 0.88	8.72 ± 0.88	0.0	0.0
selective reaction	91.07 ± 1.00	8.54 ± 0.99	0.39 ± 0.04	4.9
complete reaction	90.41 ± 1.74	8.42 ± 1.82	1.17 ± 0.14	61.0

accurately describes the transient response of the D peak. With no additional regression, Figure 2a compares the predicted model curve and experimental data.

The ratio of the D peak intensity to the G peak intensity (D/G) represents a characteristic number of defects for a SWNT sample.[21] XPS was conducted on samples representing no reaction, selective reaction, several extents of nonselective reaction, and complete (nonselective) reaction to determine the corresponding extent of functionalization (moles of chlorine per mole of carbon). For the nonselective reactions, a single addition of reagent was made and allowed to react nonselectively. For the complete, nonselective reaction, excess reagent was added. Figure 4c illustrates an increasing D/G ratio with increasing diazonium added for nonselective reactions.

Table 1 reports a maximum chlorine atomic concentration of 1.2% under nonselective, complete functionalization conditions. It is important to note that the contribution of amorphous carbon and other impurities to the carbon peak could not be distinguished from the SWNT contribution. This suggests a surface coverage of one diazonium moiety per 100 carbons. For the (10,10) nanotube, which has approximately 40 carbons per nanometer, this predicts one diazonium addend per 2.5 nm of SWNTs. The ratio of the D peak to G peak intensities increases by a factor of 15 in this case.

The PL response is accurately described by a simple linear combination of B[t] and C[t]$^{0.4}$ with no additional modifications to the model. Both types of defects (covalent C[t] and noncovalent B[t]) are known to diminish the PL intensity.[23] The former localizes electrons within the covalent bonds, altering the local band structure, while the latter creates impurity states near the band edge. Both are observed as attenuation in photoabsorption and photoluminescence. The photoluminescence attenuation can be predicted as a linear combination of the covalent and noncovalent behaviors. Figure 2c compares the experimental data to predicted trends for the PL of the (6,5) and (7,5) nanotubes with $[\alpha B[t] + (1 - \alpha)C[t]^{0.4}]$, with $\alpha = 0.81$. In this model, α represents the relative sensitivity of the nanotube to noncovalent defects; therefore, if $\alpha = 0$, the photoluminescence will behave in the same way as the D peak. Experimental data and trends were also generated for the (10,2) and (8,3) nanotubes (Supporting Information).

Additional Evidence for the Two-Step Mechanism. Supporting evidence for the presence of a stable, long-lived, and noncovalently bound intermediate is obtained by comparing the amount of reagent added to the resulting covalent coverage obtained via XPS. Survey scans of completely functionalized SWNT show the presence of chlorine, carbon, and oxygen (Supporting Information). Oxygen is present at approximately 10 and 9 mol % in the HiPco raw material and after processing,[18] respectively, presumably as a combination of pre-adsorbed oxygen and carboxyl functionalities as identified in earlier work.[23,28,29]

Table 1 is a summary of compositions for unreacted, selectively reacted, and completely (nonselectively) reacted SWNT samples determined by XPS. This table compares the atomic chlorine concentration detected on a reacted solid sample (following rigorous washing) to its predicted value based on a mass balance on the reactor. The results indicate that less than 10% of the reagent actually forms a covalent bond with the nanotube. Noncovalently bound reagent (B[t]) comes from the resulting population of unattached reagent. A comparison between a selective reaction (only metallic features significantly affected) and complete reaction (all features affected) shows that the chlorine concentration for a selectively reacted sample is roughly 33% of that observed from a completely reacted sample (0.4% versus 1.2%). Since HiPco samples are typically 33% metallic, this corresponds to "complete reaction" of the metallic nanotubes.

Also, blocking the covalent pathway can isolate the effect of the initial adsorption step and confirm the existence of the two-step mechanism. We demonstrate this by changing surfactant systems from sodium dodecyl sulfate to sodium cholate. The latter has a much smaller self-aggregation tendency (2−4 monomers per micelle compared to 30−40 monomers per micelle for SDS) and a curvature that should yield a tighter coverage at the nanotube surface[30] (Figure 5a,b).

It is proposed that SDS creates a beaded structure at the nanotube surface with a period similar to that found for SDS adsorbed on graphite (5.0−5.2 nm).[31,32] Figure 5b illustrates a geometry-optimized representation of a beaded SDS structure on the surface of a (10,10) nanotube with a periodicity of approximately 4.5−4.8 nm. Based on this model, there is a negatively charged, 0.5−0.7 nm band on the nanotube surface between SDS beads available for reaction with the positively charged diazonium. From XPS, we know that for a (10,10) nanotube there is approximately one diazonium moiety per 2.5 nm at complete conversion. Note that the XPS results agree with our surfactant model as they indicate that complete functionalization requires two addends per SDS bead (≈5 nm). The sodium cholate/SWNT molecular model (Figure 5b) shows only small (approximately 0.06 nm^2) areas available to the diazonium reagent.

Experimentally, the increased coverage of sodium cholate eliminates covalent reaction from the 4-chlorobenzene diazonium pathway, but the initial adsorption/doping step is still active. Figure 5d presents transient photoabsorption data after addition of 1.5 mM 4-chlorobenzene diazonium reagent to 2 wt % sodium cholate suspended carbon nanotubes. Figure 5e shows the Raman spectrum (785 nm) of the cholate/SWNT solution initially and after 150 min. The diminution of the absorption peaks combined with the partial reduction of photoluminescence and G peak and the absence of a significant

(28) Chen, J.; Hamon, M. A.; Hu, H.; Chen, Y. S.; Rao, A. M.; Eklund, P. C.; Haddon, R. C. *Science* **1998**, *282*, 95−98.
(29) Okpalugo, T. I. T.; Papakonstantinou, P.; Murphy, H.; McLaughlin, J.; Brown, N. M. D. *Carbon* **2005**, *43*, 153−161.
(30) Nair, P. P. *The bile acids; chemistry, physiology, and metabolism*; Plenum Press: New York, 1971; Vol. 1.
(31) Islam, M. F.; Rojas, E.; Bergey, D. M.; Johnson, A. T.; Yodh, A. G. *Nano Lett.* **2003**, *3*, 269−273.
(32) Wanless, E. J.; Ducker, W. A. *J. Phys. Chem.* **1996**, *100*, 3207−3214.

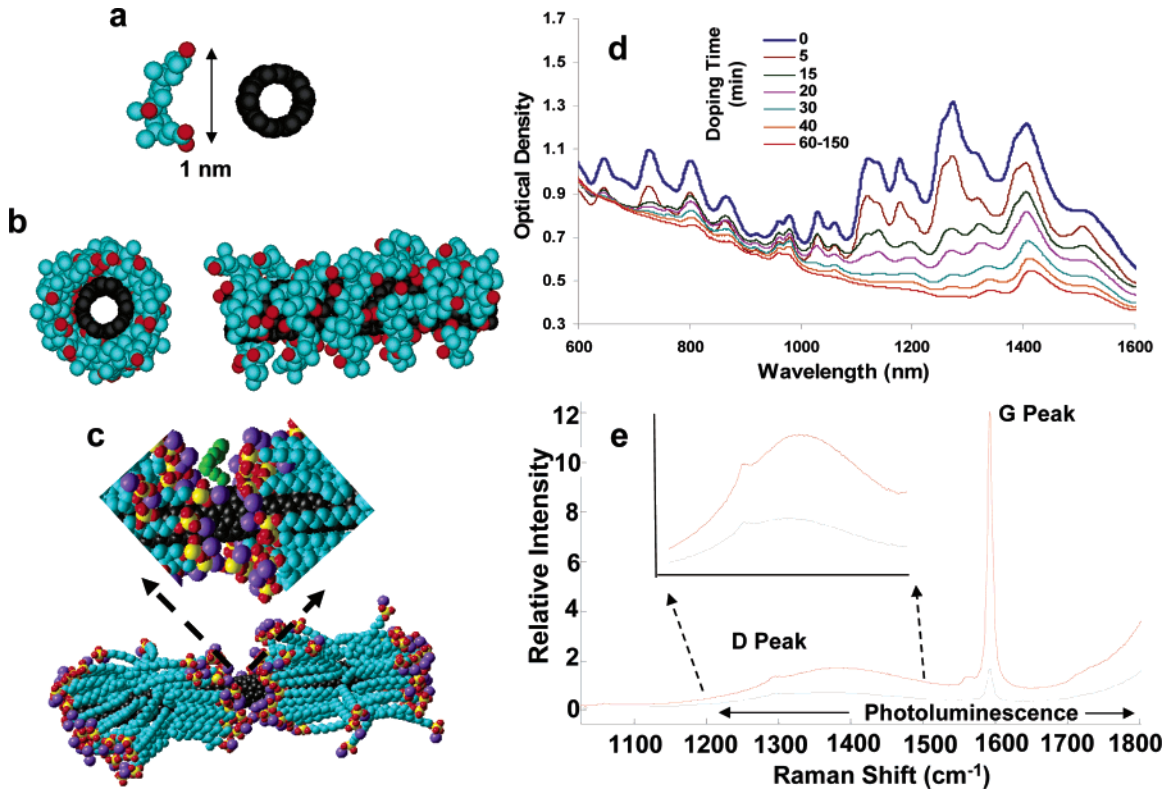

Figure 5. Molecular models of surfactant-assembled SWNTs in an aqueous dispersion: (a) sodium cholate next to SWNTs showing similarity in radius of curvature, (b) sodium cholate assembled on SWNT surface, and (c) sodium dodecyl sulfate assembled on SWNT surface showing a close-up of the diazonium reagent (green) at the available reactive site. Results of functionalization of sodium cholate suspended SWNTs with 4-chlorobenzene diazonium. (d) Transient absorption spectra taken after 1.5 mM addition showing the decrease in absorption Van Hove singularities with increasing doping time. (e) Raman spectrum of solution before (red line) and following 150 min (gray line) showing no covalent reaction.

D peak indicates SWNT doping via reagent adsorption, but no covalent reaction.

Moreover, it is the absorption interaction that appears to be selective to nanotube band-gap as in the case of noncovalent reaction with (H^+), with the greatest diminution occurring for larger band-gap species (<1300 nm).[22] The smallest band-gap nanotubes in the sample (>1300 nm) do not exhibit complete doping, which may reflect the combined steric influence of the surfactant and the smaller diameter of these nanotubes. Recent findings by Doorn and co-workers indicate that the reactivity of a small organic electron-acceptor molecule undergoing redox doping with a nanotube via electron transfer is dependent upon the chirality and band-gap of the nanotube.[33] Reactivity via electron transfer diminishes when the redox potential of the organic acceptor overlaps with the relative potential energy of the nanotube valence band. Additional bleaching is attributed to excited-state quenching due to higher acceptor concentrations. Reduction potentials for diazonium salts are typically very low (−0.18 to 0.37 V/SCE);[34,35] however, there is no published value for 4-chlorobenzene diazonium. As a result, a direct comparison between the nanotube valence band potential energies and the reduction potential of this reagent is not possible. However, as reduction potentials for diazonium salts are very similar to those of the organic acceptors utilized by Doorn and co-workers, similar chiral-selective redox doping is assumed.

The fact that the first step in the mechanism is selective resolves the dilemma of local versus delocalized reactivity. The selective step is a noncovalent charge transfer via a mechanism known to be more reactive for metallic over semiconducting nanotubes. Once the reagent has adsorbed preferentially on the nanotube, the covalent step can proceed nonselectively and even according to pyrimidization and not change the ultimate result. In a subsequent publication we will explore the implications of this in more detail.

Conclusion

In conclusion, the selective reaction of 4-chlorobenzene diazonium with SWNTs suspended in SDS aqueous solution was examined using Raman spectroscopy (785 nm) and photoluminescence in real time. A characteristic two-step mechanism consisting of a fast selective noncovalent adsorption followed by a slower covalent reaction that need not be selective was identified. Distinct time constants were determined for each step by fitting experimental data to a series of two first-order reactions representing the adsorption and reaction, respectively. During the "fast" step ($\tau = 2.4$ min), a long-lived intermediate selectively binds noncovalently to the nanotube surface, resulting in a partial doping. This step is represented by the initial response of the G peak (~1590 cm^{-1}). During the "slow" step ($\tau = 73$ min), the nonselective covalent reaction occurs. This step is represented by the restoration of the G peak and the increase of the D peak (~1300 cm^{-1}). The photoluminescence response is modeled by a combination of these responses as both adsorption and reaction diminish PL intensity. The covalent

(33) O'Connell, M. J.; Eibergen, E. E.; Doorn, S. K. *Nat. Mater.* **2005**, *4*, 412−418.
(34) Allongue, P.; Delamar, M.; Desbat, B.; Fagebaume, O.; Hitmi, R.; Pinson, J.; Saveant, J. M. *J. Am. Chem. Soc.* **1997**, *119*, 201−207.
(35) Pinson, J.; Podvorica, F. *Chem. Soc. Rev.* **2005**, *34*, 429−439.

reaction step can be prevented by changing the surfactant from sodium dodecyl sulfate to sodium cholate.

This study represents the first determination of a mechanism for an electronic structure-selective reaction in SWNT systems. This two-step mechanism explains how delocalized electrons allow the reagent to detect the electronic structure of the nanotube during adsorption before becoming localized following covalent reaction.

Acknowledgment. The authors acknowledge funding for this work from NSF NIRT ECS 04-03489. M.S.S. is grateful for an NSF Career Award. The authors thank M. Shim for insightful discussions. X-ray photoelectron spectroscopy analysis was carried out in the Center for Microanalysis of Materials, University of Illinois, which is partially supported by the U.S. Department of Energy under grant DEFG02-91-ER45439. The authors thank Rick Haasch for his assistance with the Kratos Axis Ultra instrument.

Supporting Information Available: Photoluminescence data and models for transient behavior of (10,2) and (8,3) nanotube; XPS survey of completely functionalized SWNT solid; discussion of nonlinear dependence of D peak intensity on concentration of defects (C). This material is available free of charge via the Internet at http://pubs.acs.org.

JA0537530